Progress In Electromagnetics Research M, Vol. 68, 109–117, 2018

Semi-Analytical Model for Skewed Magnet Axial Flux Machine

Md M. Reza* **and Rakesh K. Srivastava**

Abstract—High power density and torque capability are distinguished features of slotted axial flux permanent magnet machine. However, due to alternate placement of slot and teeth, the airgap permeance and airgap magnetic energy vary with angular position. Even in absence of current excitation, the magnetic variation with position results in cogging torque. This torque produces several undesirable phenomena such as mechanical vibration, acoustic noise, torque ripples, voltage ripples and speed ripple in machine performance. The severity is high for low speed, light load, and direct drive applications. Various design modifications such as slot skewing, magnet skewing, axillary slots, optimization of pole pitch to pole arc ratio and many more are reported for cogging torque mitigation. Any of these design modifications adversely affects the machine performance in terms of no load magnetic field distribution, linkage flux, and induced emf. In this paper, the effect of magnet skewing is investigated for dual-rotor permanent magnet axial flux machine. The analytical model is developed for the determination of magnetic field distribution at no load. Three different types of open slots stators viz. type 1: trapezoidal Slot with trapezoidal teeth, type 2: Parallel slot with trapezoidal teeth, and type 3: trapezoidal slot with parallel teeth are used for the investigation of air-gap magnetic field density and cogging torque produced in machine. The analytically obtained results are compared with finite element analysis (FEA) for the validation.

1. INTRODUCTION

Permanent magnet (PM) machines are gaining popularity because of their distinguished features such high power density, power factor, efficiency, and torque density. Advancement in research of permanent magnet and power electronics is enhancing the application range of PM machines. However, due to alternate placement of slot and teeth, the airgap permeance and airgap magnetic energy vary with angular position. Even in the absence of current excitation, the magnetic variation with position results in cogging torque. Though its resultant average value is zero, it produces several undesirable phenomena such as mechanical vibration, acoustic noise, torque ripples, voltage ripples and speed ripple in machine performance. In servo drives, it degrades the response of the high-performance motion control particularly at low speed, light load, and direct drives. Various design techniques exist for reducing the cogging torque such as magnet shifting [1], uneven distribution of slots [1, 2], uneven width of slots/teeth [2, 3], slot skewing, magnet skewing, and dummy slots on stator teeth in radial flux permanent-magnet (RFPM) machines. However, although some of them can be applied to axial-flux PM (AFPM) machines, most of them may be prohibitive due to the additional manufacturing complexity and cost. In [4, 5], the authors have analyzed cogging torque for axial machines and suggested several modifications of magnet shaping, and their analysis is based on FEM. Among all these, skewing of magnet is more suitable for axial flux permanent magnet as it can be easily achieved. From design aspects, the cogging mitigation is achieved by either varying magnetic field distribution or

Received 12 March 2018, Accepted 25 April 2018, Scheduled 9 May 2018
* Corresponding author: Md Motiur Reza (reza.motiur@gmail.com).
The authors are with the Department of Electrical Engineering, IIT BHU, Varanasi 221005, India.

slot distribution, and hence the machine performances in terms of magnetic field distribution, linkage flux, and induced emf are adversely affected.

For estimation of machine performance parameters such as cogging torque, average torque, and induced emf, knowledge of magnetic field distribution in machine is required. FEA and analytical method are common practice for field solution. The accuracy of FEA is higher than analytical one as it takes account of magnetic saturation and irregular geometry. However, the former is more time consuming and not suitable for iterative design process and optimization. Alternatively, designers mostly rely on analytical method for the first stage of design as it provides the performance of machine in terms of machine dimensions and its material properties. Moreover, it is less time consuming and sufficiently accurate. Numerous analytical approaches have been developed for the determination of slotted machine's magnetic field distribution, hence cogging torque [6–12]. These analytical methods depend on either magnetic equivalent reluctance model, conformal method, methods of images, or solution of governing equations by use of variable separable method. Magnetic equivalent reluctance model requires expertise and experience in magnetic flux prediction. Furthermore, computational complexity and inaccuracy are high especially for irregular shape of machine's geometry and magnetic saturation. In 1993 Zhu et al. [13] solved magnetic field distribution in a slotless permanent magnetic machine by use of variable separable method. Further, the authors incorporated the slotting effect using conformal mapping approach and deducted a 2D relative permeance function to account for the slotting effect [6]. However, this approach is limited to estimation of radial field only. Further improved solution is introduced by using conformal mapping [8], which takes account of radial as well as tangential flux density. The solution of slotted permanent magnetic machine is obtained by use of complex permeance function and field of slotless machine [8]. The complex permeance function was determined numerically, and it increased the complexity. Even at present, the analytical calculation of complex permeance function is still a problem of research. More accurate results are found by use of subdomain method of analysis, which solves governing equations in all subdomain including slots, air gap, and magnets region [10–12]. Most of these analytical methods are applicable to axial flux permanent magnet machines.

In this paper, analytical solution of skewed magnet axial flux machine is developed. This method uses combination of multislice method and subdomain analysis method. Multislice method reduces the complexity of problem by converting a three-dimensional field problem to two-dimensional one. The effect of skewed magnet is taken by use of relative shifting of direct axis. Analytically achieved field solution is validated with FEM results.

2. ANALYTICAL ANALYSIS

2.1. Analytical Prediction of No Load Magnetic Field

A dual-rotor permanent magnet machine with skewed magnets shown in Fig. 1 is investigated analytically. The axial flux machine with skewed magnet rotor and unskewed magnet rotor are depicted in Fig. 2. In magnet skewed machine, the location of direct axis of magnet shifts gradually in peripheral direction, as it is traced from inner radius to outer radius of rotor core as shown in Fig. 3. The machine is divided into a certain number of annular slices in the radial direction. The direct axis of each slice is displaced by a certain angle. The analytical model is based on the solution of Maxwell equations, and it is established at the average radius of each slice. The multislice approach takes the accountability of 3D up to certain extent. The 2-dimensional model achieved by unrolling an infinitesimally small thick slice at radius r is shown in Fig. 4. The complete 3D model is considered as comprising infinite many slice models, which differ from each other by a rotational angle. The slice model present at an arbitrary radius r is displaced with a slice model at inner radius R_i by θ_i, which is defined as $\theta_i = \theta_s(r - R_i)/r$, where θ_s is the skewed angle. The magnetic field of this slice located at radius r is established. To establish analytical solution, the following assumption has been made

(i) Stator is assumed to unsaturated, and hence the relative permeability is assumed constant.

(ii) Radial magnetic flux has been ignored. However, the radial fringing is accounted by use of correction factor.

(iii) Magnet's demagnetization curve is straight.

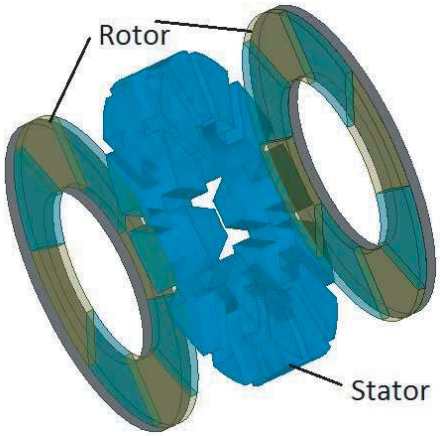

Figure 1. Axial flux permanent magnet machine.

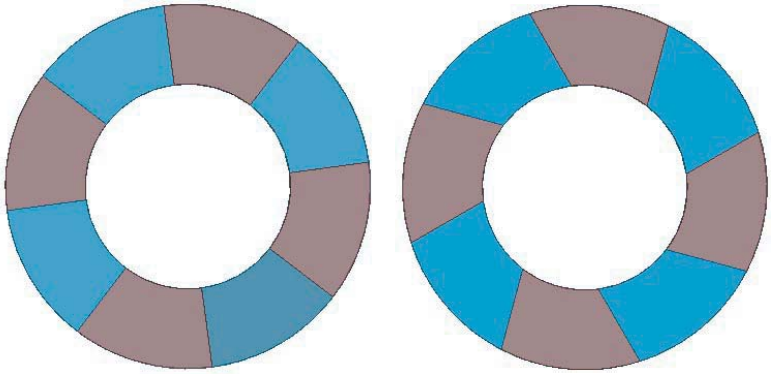

Figure 2. Axial flux permanent machine's rotor. (a) Unskewed rotor. (b) Skewed rotor.

Due to symmetry of the linear model shown in Fig. 4, half of the model is analyzed. With consideration of above assumptions, the simplified 2-dimensional model is as shown in Fig. 5. The magnetic field analysis is confined to $(Qs + 2)$ regions viz. region 1j, where i is the number of slots, air-gap II, and permanent magnet region III. For the permanent magnet machines, $\overrightarrow{B}$ and $\overrightarrow{H}$ are coupled as

$$\overrightarrow{B} = \begin{cases} \mu_0 \overrightarrow{H}_I & \text{In slot region Ij} \\ \mu_0 \overrightarrow{H}_{II} & \text{In air-gap region II} \\ \mu_0 \mu_r \overrightarrow{H}_{III} + \mu_0 \overrightarrow{M} & \text{In PM region III} \end{cases} \tag{1}$$

where M and μ_r are the remanent magnetization and relative permeability of magnet and related to remanent flux density as $B_{rem} = \frac{M}{\mu_o}$. The magnetization distribution pattern written in rotor frame attached to direct axis of magnet at inner radius is as shown in Fig. 6, which can be expanded in Fourier series as

$$M = \sum_{n=1,3,5\ldots}^{\infty} M_n \cos np(\theta - \theta_i) \tag{2}$$

where, $M_n = \frac{4B_{rem}}{\mu_o n\pi} \sin(\frac{n\pi\alpha_p}{2})$ and α_p is the ratio of magnet pitch θ_m to pole pitch θ_p.

The governing equation for magnetic field has been formulated in terms of magnetic vector potential

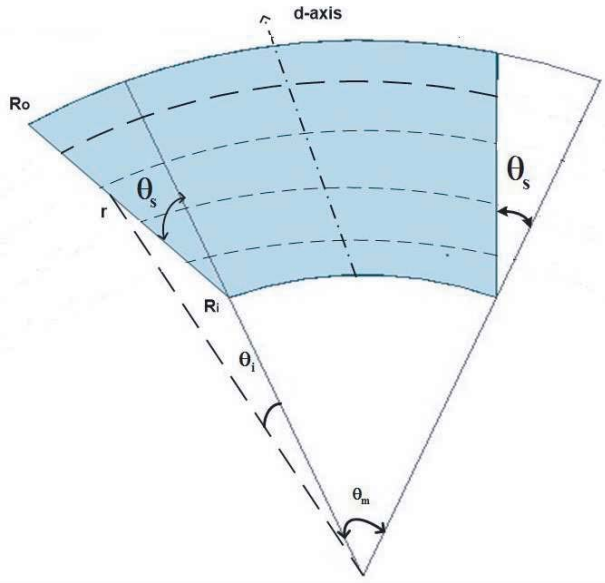

Figure 3. Rotor structure with skewed magnet.

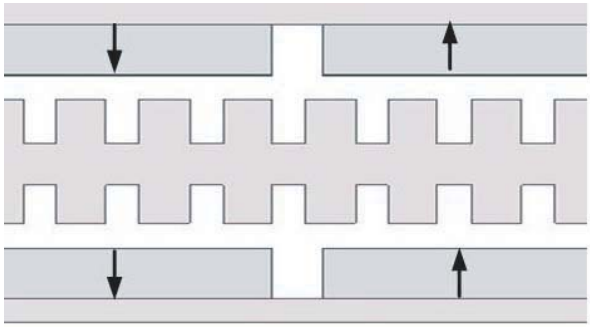

Figure 4. Unrolled portion of axial permanent magnet machine.

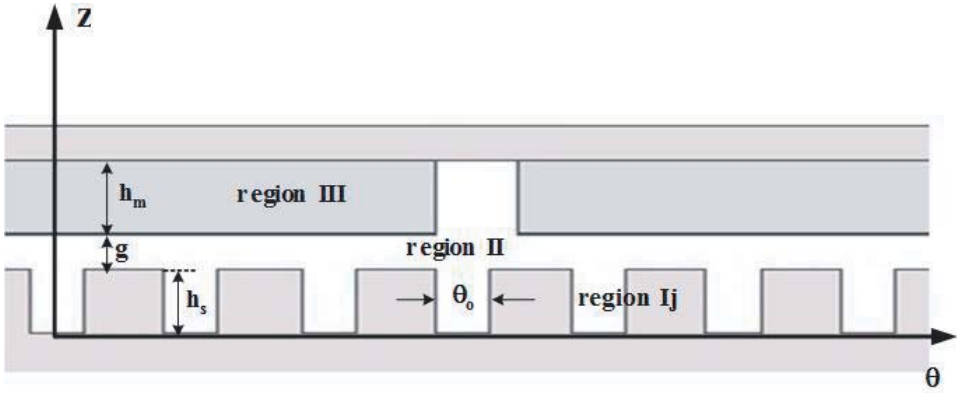

Figure 5. Unrolled portion of axial permanent magnet machine used for analytical analysis.

A defined as $\mathbf{B} = \nabla \times \mathbf{A}$.

$$\left.\begin{aligned} \mathrm{B_r} &= -\frac{\partial A_r}{r\partial\theta} \\ \mathrm{B}_\theta &= \frac{\partial A_r}{\partial z} \end{aligned}\right\} \tag{3}$$

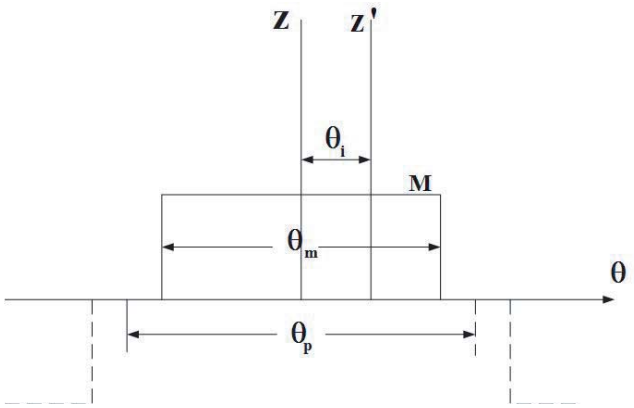

Figure 6. Magnetization distribution.

The governing field equations in all regions, in terms of Coulomb gauge, $\nabla \cdot \mathbf{A} = 0$, are

$$\nabla^2 A_r = \begin{cases} 0; & \text{region Ij} \\ 0; & \text{region II} \\ -\mu_0 \nabla \times M; & \text{region III} \end{cases} \tag{4}$$

Effectively, the governing equations in all regions can be rewritten in a coordinate frame attached with stator as

$$\left.\begin{aligned} \frac{1}{r^2}\frac{\partial A_{Ijr}}{\partial r} + \frac{1}{r}\frac{\partial^2 A_{Ijr}}{\partial \theta^2} &= 0 \\ \frac{1}{r^2}\frac{\partial A_{IIr}}{\partial r} + \frac{1}{r}\frac{\partial^2 A_{IIr}}{\partial \theta^2} &= 0 \\ \frac{1}{r^2}\frac{\partial A_{IIIr}}{\partial r} + \frac{1}{r}\frac{\partial^2 A_{IIIr}}{\partial \theta^2} &= -\frac{npP_n}{r}\sin np(\theta - \theta_i - \alpha) \end{aligned}\right\} \tag{5}$$

where α is the arbitrary location of magnet from stator coordinate frame, and $P_n = \frac{4B_{rem}}{n\pi}\sin(\frac{n\pi\alpha_p}{2})$. The boundary conditions to be satisfied by solution of above partial differential equations are

$$\begin{aligned} &B_{Ij\theta}(\theta, z)|_{z=0} = 0; \quad B_{Ijz} = B_{2z}|_{z=h_s}; \quad B_{IIz} = B_{IIIz}|_{z=(h_s+g)} \\ &H_{II\theta} = H_{III\theta}|_{z=(h_s+g)}; \quad B_{III\theta}(\theta, z)|_{z=(h_s+g+h_m)} = 0 \\ &B_{Ijz}(\theta, z) = 0; \quad \forall \ \theta \in \left\{-\frac{\theta_o}{2} + \frac{2\pi j}{Q_s}, \frac{\theta_o}{2} + \frac{2\pi j}{Q_s}\right\} \\ &H_{II\theta}|_{z=h_s} = \begin{cases} H_{Ij\theta}; & \forall \ \theta \in \left[-\frac{\theta_o}{2} + \frac{2\pi j}{Q_s}, \frac{\theta_o}{2} + \frac{2\pi j}{Q_s}\right] \\ 0; & \forall \ \theta \notin \left[-\frac{\varphi_o}{2} + \frac{2\pi j}{Q_s}, \frac{\varphi o}{2} + \frac{2\pi j}{Q_s}\right] \end{cases} \end{aligned} \tag{6}$$

The air-gap magnetic field distributions are given as

$$\begin{aligned} B_{IIz}(z,\theta) \ = \ &\sum_{n=1}^{\infty}\left\{a_{IIn}\sinh\left(\frac{npz}{r}\right) + b_{IIn}\cosh\left(\frac{npz}{r}\right)\right\}\sin np\theta \\ &-\sum_{n=1}^{\infty}\left\{c_{IIn}\sinh\left(\frac{npz}{r}\right) + d_{IIn}\cosh\left(\frac{npz}{r}\right)\right\}\cos np\theta \end{aligned} \tag{7}$$

and

$$\begin{aligned} B_{II\theta}(z,\theta) \ = \ &\sum_{n=1}^{\infty}\left\{a_{IIn}\sinh\left(\frac{npz}{r}\right) + b_{IIn}\cosh\left(\frac{npz}{r}\right)\right\}\cos np\theta \\ &+\sum_{n=1}^{\infty}\left\{c_{IIn}\sinh\left(\frac{npz}{r}\right) + d_{IIn}\cosh\left(\frac{npz}{r}\right)\right\}\sin np\theta \end{aligned} \tag{8}$$

a_{IIn}, b_{IIn}, c_{IIn}, and d_{IIn} are the coefficients involved in 7 and 8 determined by the boundary conditions 6 on the interface between the subdomains [14].

2.2. Cogging Torque Calculation

The cogging torque is calculated by use of Maxwell stress tensor [14]

$$T = \frac{1}{\mu_o} \iint_S r B_{IIz} B_{II\theta} ds \tag{9}$$

where B_{IIz} and $B_{II\theta}$ are axial and tangential flux densities at magnet surface, and S is the PM's surface and defined as $ds = rdrd\theta$, which is further simplified as

$$T_{cog} = \frac{1}{\mu_o} \int_0^{2\pi} \int_{r_i}^{r_o} B_{IIz} B_{II\theta} r^2 dr d\theta \tag{10}$$

For multislice modeling of axial flux machine, the total cogging developed in machine is calculated as algebraic summation of cogging torque produced due to each slice.

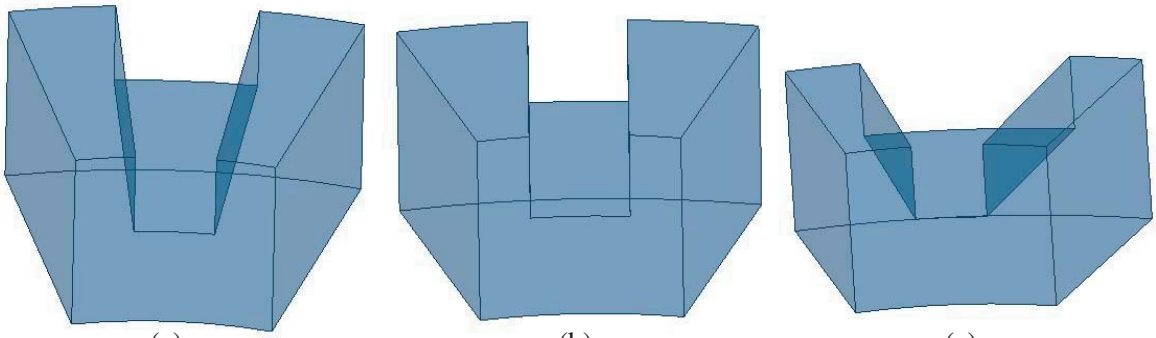

Figure 7. Axial flux permanent machine's slot type. (a) Type 1: Trapezoidal slot with trapezoidal teeth, (b) type 2: Parallel slot with trapezoidal teeth, and (c) type 3: Trapezoidal slot with parallel teeth.

Table 1. Parameters of machines.

Machine's Parameters	Values
No of poles (p)	8
No of Slots (Q_s)	12
Slot Height (h_s)	10 mm
Inner Radius (R_i)	45 mm
Outer Radius (R_o)	90 mm
Magnet Height (h_m)	4 mm
Magnet Pitch θ_m	$\pi/4$
Magnet Skewed Angle θ_s	$\pi/12$
Air gap (g)	1 mm
Slots Width at $r = R_i, \theta_o$	12° (type 1), 12° (type 2), 12° (type 3)
Slots Width at $r = R_o, \theta_o$	12° (type 1), 6.75° (type 2), 19.875° (type 3)
B_r, μ_r	1.1 T, 1.05

3. FINITE ELEMENT ANALYSIS AND ANALYTICAL RESULTS COMPARISON

The developed analytical solution is verified with finite element analysis (FEA). The FEA is obtained by use of 3D modeling in Ansys Maxwell software. Three different shapes of open slots viz. type 1: trapezoidal Slot with trapezoidal teeth, type 2: parallel slot with trapezoidal teeth, and type 3: trapezoidal slot with parallel teeth as shown in Fig. 7 are considered for no load magnetic field and cogging torque investigation. Slot's crosssectional area varies with radius with minimum area at inner radius. To maintain constant electrical loading of machine, the slot areas for all slot types are kept constant. The machine dimension used for the analytical analysis and its FEM verification are given in Table 1. The air-gap magnetic flux density distribution is obtained analytically and compared with FEA results. The flux densities at $z = 9.5\,\text{mm}$ with different radial distances at $r = 55\,\text{mm}$ and $r = 70\,\text{mm}$ are plotted in Fig. 8. The shift of magnet axis along with radial distance is shown in Fig. 8 due to magnet skewing and is reflected in the analytical and FEA both results. For type 1 slot, the slot opening is 12° at every radius, while for the second type of slot, i.e., parallel slot, slot opening angle θ_o decreases with radius as shown in Fig. 8(b). Moreover, for type 2 kind of slots, the opening angle increases with radius, shown in Fig. 8(c). Due to trapezoidal slot and teeth shape of type 1 slot, and trapezoidal shape of skewed magnet, the cogging torque of type 1 is the highest among them. Fig. 9 shows the cogging torque calculated analytically and compared with FEA for all types of slot's shape.

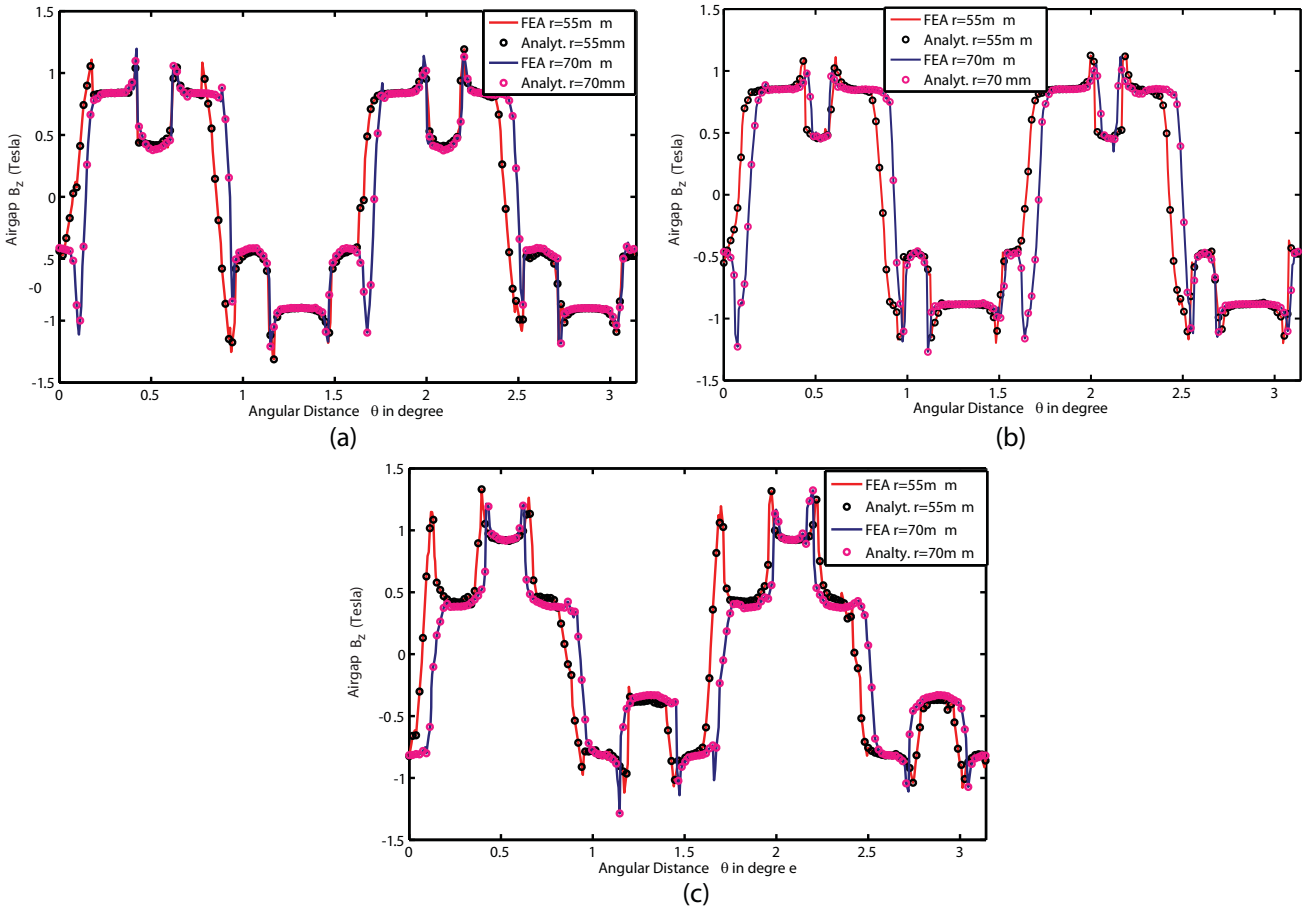

Figure 8. Comparison of air-gap ($z = 9.5\,\text{mm}$) axial flux density component at different radial $r = 55\,\text{mm}$, and $r = 70\,\text{mm}$ location of skewed magnet machines. (a) Type 1: Trapezoidal slot with trapezoidal teeth , (b) type 2: Parallel slot with trapezoidal teeth, and (c) type 3: Trapezoidal slot with parallel teeth.

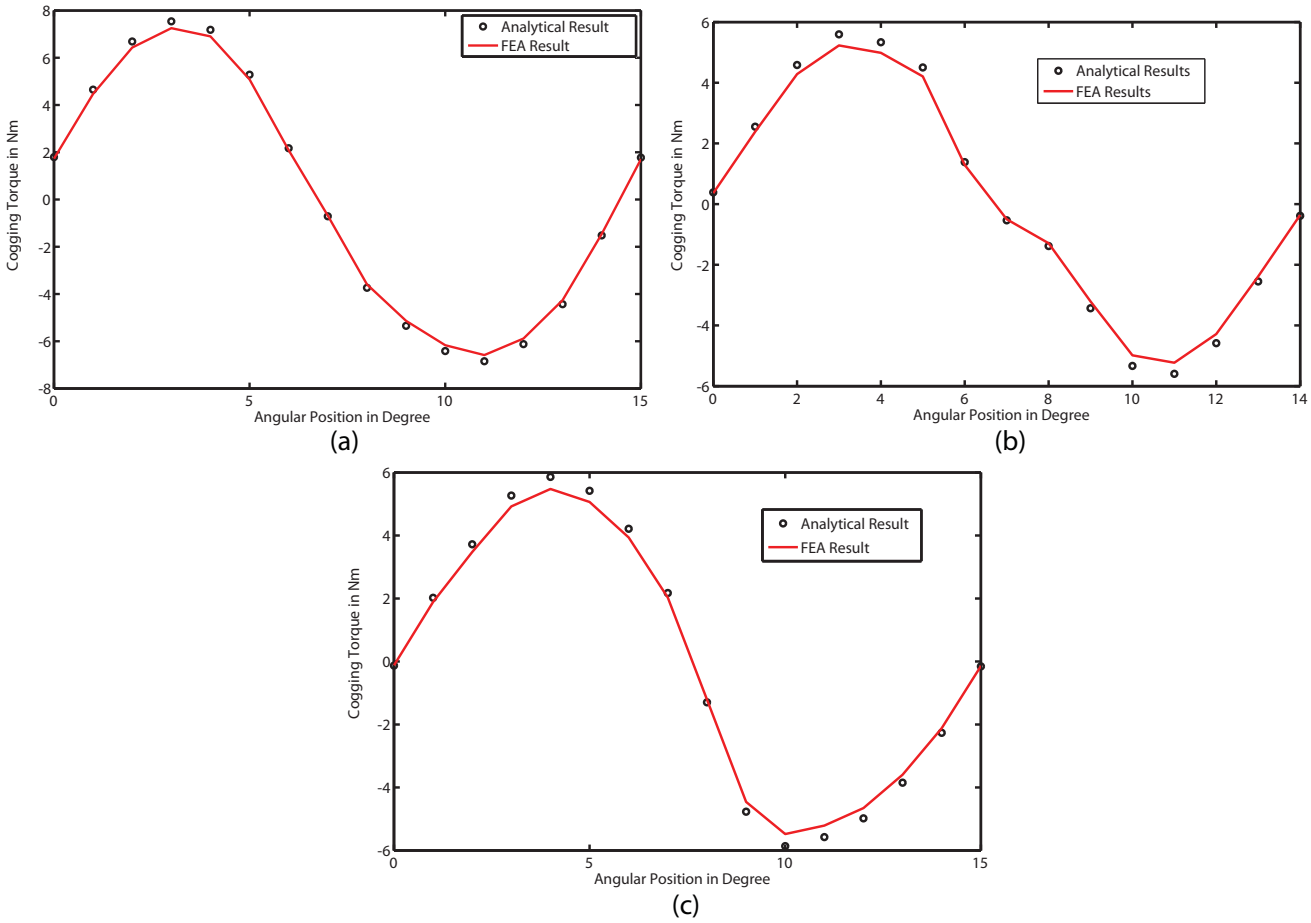

Figure 9. Comparison of analytical and FEA cogging torque of skewed magnet machines. (a) Type 1: Trapezoidal slot with trapezoidal teeth, (b) type 2: Parallel slot with trapezoidal teeth, and (c) type 3: Trapezoidal slot with parallel teeth.

4. CONCLUSION

Analytical model for skewed magnet axial flux machine for the magnetic field calculation has been derived. The analysis has been validated by finite element method calculations. Due to magnet skewing the direct axis of magnet shifts in the direction of magnet skewing. A close agreement between the results obtained by these two methods confirms the effectiveness and accuracy of the analysis. Therefore, there is no need to apply either time consuming 3D-FEA or complex 3D analytical solution. Three different open slot shapes are analyzed and compared with FEA. The cogging torque is calculated for all of them, and it is found that the cogging of trapezoidal slot with trapezoidal tooth is the highest, while it is the lowest for trapezoidal slot with parallel teeth. The evaluated air-gap magnetic field could be further used to predict machine performance such as back emf and electromagnetic torque. The skewing effects of the magnet is accounted analytically using combined approach of the multi-slice and subdomain methods. The same method could be used for the analysis of a class of axial permanent magnet machines with different shapes of magnet and stator slot variation.

REFERENCES

1. Zhu, Z. and D. Howe, "Analytical prediction of the cogging torque in radial-field permanent magnet brushless motors," *IEEE Transactions on Magnetics*, Vol. 28, No. 2, 1371–1374, 1992.

2. Wu, L., Z. Zhu, D. Staton, M. Popescu, and D. Hawkins, "Analytical cogging torque prediction for surface-mounted pm machines accounting for different slot sizes and uneven positions," *2011 IEEE International Electric Machines & Drives Conference (IEMDC)*, 1322–1327, IEEE, 2011.
3. Wang, D., X. Wang, D. Qiao, Y. Pei, and S.-Y. Jung, "Reducing cogging torque in surface-mounted permanent-magnet motors by nonuniformly distributed teeth method," *IEEE Transactions on Magnetics*, Vol. 47, No. 9, 2231–2239, 2011.
4. Aydin, M., Z. Zhu, T. Lipo, and D. Howe, "Minimization of cogging torque in axial-flux permanent-magnet machines: Design concepts," *IEEE Transactions on Magnetics*, Vol. 43, No. 9, 3614–3622, 2007.
5. González, D. A., J. A. Tapia, and A. L. Bettancourt, "Design consideration to reduce cogging torque in axial flux permanent-magnet machines," *IEEE Transactions on Magnetics*, Vol. 43, No. 8, 3435–3440, 2007.
6. Zhu, Z. and D. Howe, "Instantaneous magnetic field distribution in brushless permanent magnet dc motors. iii. Effect of stator slotting," *IEEE Transactions on Magnetics*, Vol. 29, No. 1, 143–151, 1993.
7. Zhu, Z. and D. Howe, "Instantaneous magnetic field distribution in permanent magnet brushless dc motors. iv. Magnetic field on load," *IEEE Transactions on Magnetics*, Vol. 29, No. 1, 152–158, 1993.
8. Zarko, D., D. Ban, and T. A. Lipo, "Analytical calculation of magnetic field distribution in the slotted air gap of a surface permanent-magnet motor using complex relative air-gap permeance," *IEEE Transactions on Magnetics*, Vol. 42, No. 7, 1828–1837, 2006.
9. Zarko, D., D. Ban, and T. A. Lipo, "Analytical solution for cogging torque in surface permanent-magnet motors using conformal mapping," *IEEE Transactions on Magnetics*, Vol. 44, No. 1, 52–65, 2008.
10. Dubas, F. and C. Espanet, "Analytical solution of the magnetic field in permanent-magnet motors taking into account slotting effect: No-load vector potential and flux density calculation," *IEEE Transactions on Magnetics*, Vol. 45, No. 5, 2097–2109, 2009.
11. Lubin, T., S. Mezani, and A. Rezzoug, "2-d exact analytical model for surface-mounted permanent-magnet motors with semi-closed slots," *IEEE Transactions on Magnetics*, Vol. 47, No. 2, 479–492, 2011.
12. Zhu, Z., L. Wu, and Z. Xia, "An accurate subdomain model for magnetic field computation in slotted surface-mounted permanent-magnet machines," *IEEE Transactions on Magnetics*, Vol. 46, No. 4, 1100–1115, 2010.
13. Zhu, Z., D. Howe, E. Bolte, and B. Ackermann, "Instantaneous magnetic field distribution in brushless permanent magnet dc motors. i. Open-circuit field," *IEEE Transactions on Magnetics*, Vol. 29, No. 1, 124–135, 1993.
14. Azzouzi, J., G. Barakat, and B. Dakyo, "Quasi-3-d analytical modeling of the magnetic field of an axial flux permanent-magnet synchronous machine," *IEEE Transactions on Energy Conversion*, Vol. 20, No. 4, 746–752, 2005.